

Surface defects, stress evolution, and laser damage enhancement mechanism of fused silica under oxygen-enriched condition

Wei-Yuan Luo(罗韦媛), Wen-Feng Sun(孙文丰), Bo Li(黎波), Xia Xiang(向霞), Xiao-Long Jiang(蒋晓龙),Wei Liao(廖威), Hai-Jun Wang(王海军), Xiao-Dong Yuan(袁晓东),Xiao-Dong Jiang(蒋晓东), and Xiao-Tao Zu(祖小涛)

Citation: Chin. Phys. B, 2022, 31 (**5**): 054214. DOI: 10.1088/1674-1056/ac5a3e
Journal homepage: http://cpb.iphy.ac.cn; http://iopscience.iop.org/cpb

What follows is a list of articles you may be interested in

Variation of electron density in spectral broadening process in solid thin plates at 400 nm

Si-Yuan Xu(许思源), Yi-Tan Gao(高亦谈), Xiao-Xian Zhu(朱孝先), Kun Zhao(赵昆), Jiang-Feng Zhu(朱江峰), and Zhi-Yi Wei(魏志义)

Chin. Phys. B, 2021, 30 (**10**): 104205. DOI: 10.1088/1674-1056/abf0fe

Optical modulation of repaired damage site on fused silica produced by CO_2 laser rapid ablation mitigation

Chao Tan(谭超), Lin-Jie Zhao(赵林杰), Ming-Jun Chen(陈明君), Jian Cheng(程健), Zhao-Yang Yin(尹朝阳), Qi Liu(刘启), Hao Yang(杨浩), Wei Liao(廖威)

Chin. Phys. B, 2020, 29 (**5**): 054209. DOI: 10.1088/1674-1056/ab8206

Damage threshold influenced by polishing imperfection distribution under 355-nm laser irradiation

Zhen Yu(余振), Hong-Ji Qi(齐红基), Wei-Li Zhang(张伟丽), Hu Wang(王虎), Bin Wang(王斌), Yue-Liang Wang(王岳亮), Hao-Peng Huang(黄昊鹏)

Chin. Phys. B, 2017, 26 (**10**): 104210. DOI: 10.1088/1674-1056/26/10/104210

Intense supercontinuum generation in the near-ultraviolet range from a 400-nm femtosecond laser filament array in fused silica

Dongwei Li(李东伟), Lanzhi Zhang(张兰芝), Saba Zafar, He Song(宋鹤), Zuoqiang Hao(郝作强), Tingting Xi(奚婷婷), Xun Gao(高勋), Jingquan Lin(林景全)

Chin. Phys. B, 2017, 26 (**7**): 074213. DOI: 10.1088/1674-1056/26/7/074213

Effects of annealing time on the structure, morphology and stress of gold-chromium bilayer film

Hong Zhang(张洪), Yun-Xia Jin(晋云霞), Hu Wang(王虎), Fang-Yu Kong(孔钒宇), Hao-Peng Huang(黄昊鹏), Yun Cui(崔云)

Chin. Phys. B, 2016, 25 (**10**): 104205. DOI: 10.1088/1674-1056/25/10/104205

Surface defects, stress evolution, and laser damage enhancement mechanism of fused silica under oxygen-enriched condition

Wei-Yuan Luo(罗韦媛)[1], Wen-Feng Sun(孙文丰)[1], Bo Li(黎波)[1,†], Xia Xiang(向霞)[1,‡], Xiao-Long Jiang(蒋晓龙)[2], Wei Liao(廖威)[2], Hai-Jun Wang(王海军)[2], Xiao-Dong Yuan(袁晓东)[2], Xiao-Dong Jiang(蒋晓东)[2], and Xiao-Tao Zu(祖小涛)[1]

[1] *School of Physics, University of Electronic Science and Technology of China, Chengdu* 610054, *China*
[2] *Research Center of Laser Fusion, China Academy of Engineering Physics, Mianyang* 621900, *China*

(Received 21 January 2021; revised manuscript received 25 February 2022; accepted manuscript online 3 March 2022)

Oxygen ions (O^+) were implanted into fused silica at a fixed fluence of 1×10^{17} ions/cm^2 with different ion energies ranging from 10 keV to 60 keV. The surface roughness, optical properties, mechanical properties and laser damage performance of fused silica were investigated to understand the effect of oxygen ion implantation on laser damage resistance of fused silica. The ion implantation accompanied with sputtering effect can passivate the sub-/surface defects to reduce the surface roughness and improve the surface quality slightly. The implanted oxygen ions can combine with the structural defects (ODCs and E′ centers) to reduce the defect densities and compensate the loss of oxygen in fused silica surface under laser irradiation. Furthermore, oxygen ion implantation can reduce the Si–O–Si bond angle and densify the surface structure, thus introducing compressive stress in the surface to strengthen the surface of fused silica. Therefore, the laser induced damage threshold of fused silica increases and the damage growth coefficient decreases when ion energy up to 30 keV. However, at higher ion energy, the sputtering effect is weakened and implantation becomes dominant, which leads to the surface roughness increase slightly. In addition, excessive energy aggravates the breaking of Si–O bonds. At the same time, the density of structural defects increases and the compressive stress decreases. These will degrade the laser laser-damage resistance of fused silica. The results indicate that oxygen ion implantation with appropriate ion energy is helpful to improve the damage resistance capability of fused silica components.

Keywords: fused silica, oxygen ion implantation, defect, mechanical property, laser damage performance

PACS: 42.70.Ce, 68.35.Dv, 78.68.+m, 81.65.−b **DOI:** 10.1088/1674-1056/ac5a3e

1. Introduction

Fused silica material with excellent optical properties, mechanical properties and thermal stability, is widely used to fabricate optical components, such as windows and lenses, in inertial confinement fusion (ICF) facilities (e.g., SG-III laser facility, National Ignition Facility (NIF) and Laser MegaJoule (LMJ)).[1–3] However, during the polishing and grinding processes, a tremendous amount of metal impurities, destructive defects and structural defects are produced in the surface of fused silica, which become the main precursors of laser-induced damage in fused silica under ultraviolet laser irradiation. Therefore, the laser-induced damage threshold (LIDT) and the lifetime of fused silica components will be significantly reduced and the operational stability of high power laser facilities will also be decreased.[4–8] With the improvement of growth method and surface treatment technique of fused silica components, e.g., magnetorheological finishing (MRF), hydrofluoric acid etching, ion beam treatment and laser pretreatment, the surface contamination and sub-surface defects of fused silica are effectively restrained to enhance the LIDT of fused silica greatly, but it is still far lower than the intrinsic LIDT.[9–14] Therefore, it is in urgent to find a new way to improve the laser load capacity of fused silica components.

At present, the effect of laser radiation on fused silica has been extensively studied. Xu *et al.* studied the structural change of fused silica under the irradiation of third harmonic Nd:YAG laser. Their results indicated that the stoichiometric ratio of oxygen to silicon decrease due to the loss of oxygen, leading to the formation of oxygen vacancies and other oxygen-deficiency related defects in the surface of fused silica.[15] Stevens Kalceff *et al.* investigated the formation of structural defects in fused silica under the irradiation of high power pulsed (355 nm) laser and its effect on laser damage mechanism of fused silica. They found that the shock wave and thermal explosion produced by laser irradiation are related to the structural defects.[16] Andrejs *et al.* found that the self-trapped excitons (STEs) will be produced in fused silica due to multiphoton absorption under the irradiation of high power laser, and then the decay of STEs will result in the formation of structural defects, which leads to the change of physical properties (refractive index, density, mechanical properties, etc.) of fused silica.[17,18] Due to the ionization effect and displacement effect, the laser irradiation will cause the loss of oxygen in fused silica surface. As a result, the O/Si ratio will decrease

†Corresponding author. E-mail: libcx@uestc.edu.cn
‡Corresponding author. E-mail: xiaxiang@uestc.edu.cn

© 2022 Chinese Physical Society and IOP Publishing Ltd

and lead to the formation of various oxygen-deficiency related defects, thus deteriorating the physical properties and decreasing the laser damage performance.

Ion implantation is an effective technique for surface modification of materials, which can be used to modify the composition and structure of materials. Derryberry *et al.* observed that there are two kinds of structural defects (E′ center and peroxy radical) in the surface of amorphous silicon after oxygen ion implantation, and both the implanted oxygen ions and peroxy radicals combine with the oxygen-deficiency related defect (E′ center), reducing the concentrations of the E′ center and peroxy radical eventually.[19] Griscom *et al.* found that the implanted oxygen ions can combine with oxygen vacancy defects, resulting in the reduction of the concentration of oxygen-deficient defects. This experimental result indicated that the concentration of the oxygen vacancy defects in fused silica material can be effectively adjusted by introducing oxygen from the outside.[20] Therefore, oxygen ion implantation can effectively adjust the stoichiometry of fused silica surface, compensate the loss of oxygen under laser irradiation, and mitigate oxygen-deficiency related defects, which is a feasible method to improve the load capacity of fused silica components. However, there has no research on this.

In addition, ion implantation has an important effect on the mechanical properties of the material surface. Chinellato *et al.* found that small fluence can enhance the mechanical properties of glass implanted with argon ions.[21] Julien *et al.* investigated the influence of nitrogen ion implantation on the glass surface. The results indicated that the introduction of nitrogen ions changes the chemical composition of the glass surface, and leads to form a more compact silica network, thus improving the hardness of the material.[22] Otherwise, ion implanted glass has smaller bond angle, higher density and compressive stress, thus strengthening the surface of the material.[23,24] The mechanical properties of materials have an important influence on the LIDT of fused silica. Our previous researches indicated that argon ion implantation can lead to the reduction of Si–O–Si bond angle, the increase of surface density, the formation of compressive stress and the improvement of the mechanical properties and laser damage resistance of fused silica components.[25] Therefore, oxygen ion implantation is also expected to form compressive stress in the surface of fused silica to strengthen the surface and improve the laser damage resistance. However, there are only a few studies about the effects of surface stress state modified by oxygen ion implantation on the laser-induced damage performance of fused silica.[26]

During the ion implantation process, the sputtering effect of ion beam has a certain influence on laser damage precursors of fused silica surface, such as the removal of metal impurities and the passivation of sub-/surface defects, which also has significant effect on the laser damage performance of fused silica. The effect of oxygen ion implantation on the laser damage performance is dominated by comprehensive factors including surface quality, defects and compressive stress. Up to now, little work has been done to investigate the influence of the evolution of structural defect induced by oxygen ion implantation on the laser damage behavior of fused silica. In addition, there is also interest to study the effects of ion implantation on the mechanical properties and the surface quality of fused silica.

In this paper, fused silica samples were implanted with oxygen ions in the energy range of 10 keV–60 keV at a fixed fluence of 1×10^{17} ions/cm^2. The effects of oxygen ion implantation on surface morphology, optical properties, microstructure, mechanical properties and laser-induced damage performance have been systematically studied. The results are beneficial to develop a new idea to further improve the load capacity of fused silica components.

2. Experimental details

Seven groups of fused silica samples (Corning 7980, 30 mm × 30 mm × 4 mm) used in the experiment were grinded and polished with CeO_2 lurry from the same manufacturer. Each group contained three samples. Before ion implantation experiment, all fused silica samples were ultrasonically cleaned with deionized water and dehydrated with absolute alcohol respectively. In this work, oxygen ion implantation was performed on a multifunctional implanter with a base pressure below 2×10^{-3} Pa. During the implantation, the samples were mounted on a rotating metal plate to ensure the uniform distribution of the implanted oxygen ions. Fused silica samples were implanted at room temperature with ion energies varying from 10 keV to 60 keV at the same fluence of 1×10^{17} ions/cm^2. The oxygen ion beam flux densities during the implantation were maintained in the range of 0.78 mA/cm^2–1.05 mA/cm^2. The incident angle was fixed at 0°, i.e., perpendicular to the substrate surface.

The distributions of implanted oxygen ions and displacement damage were simulated by the Monte Carlo codes using TRIDYN software. Before and after the implantation, the intensities of implanted oxygen ions were characterized by time of flight secondary ion mass spectrometry (TOF-SIMS) using 30 keV bismuth ions (B^+) as the sputtering source. The surface morphology and roughness of the samples were observed using an atomic force microscope (Bruker Dimension Icon). Three areas of each sample were selected to measure and calculate the average value of the root-mean-square roughness (RMS). The absorption spectra of the samples were measured at the wavelength interval of 1 nm in the range from 200 nm to

800 nm by UV–Vis spectrophotometer (PE lambda 950). The photoluminescence spectra (PL) were carried out in the wavelength range of 300 nm–750 nm using a fluorescence spectrometer (FLS1000). The excitation wavelength was 240 nm. Fourier transform infrared spectra (FTIR) were characterized in the region of 550 nm–1500 nm by a Nicolet 5700 FTIR spectrophotometer. The FTIR measurement was performed in an attenuated total reflection mode. A nanoindentation instrument (NHT^2 from Anton Parr) was used to measure the mechanical properties of the sample surfaces. The depth of the indenter into the surface and the loading force during loading/unloading were recorded to obtain the load–displacement curve.

Laser damage performance tests were performed using a single longitudinal mode Q-switched Nd: YAG laser operated at 355 nm with a pulse width of 6.4 ns. The laser beam had a spatial and temporal near-Gaussian distribution with a $1/e^2$ area of 0.6 mm^2. The laser damage threshold of fused silica was determined by R-on-1 procedure.[27] 20 sites were selected randomly for each sample and the average value was taken as the final damage threshold. The growth process of damage pit was monitored by the CCD combined with optical microscope. The morphology and the area of damage pit were collected on-line and measured off-line, respectively. Then the increase of damage pit area with the number of laser irradiation pulses was obtained.

3. Results and discussion

3.1. Depth profiles

Oxygen ion implantation with ion energies varying from 10 keV to 60 keV at a fixed fluence of 1×10^{17} ions/cm^2 were simulated by TRIDYN software. The simulated results are shown in Fig. 1. Figure 1(a) illustrates the distributions of implanted oxygen ions in fused silica surfaces at different ion energies. The implanted oxygen ions follow the Gaussian distribution with the deepest depth about 400 nm. As the ion energy increases, the main distribution of implanted oxygen ions moves to the inside of fused silica substrate and becomes wider, while the maximum oxygen concentration gradually decreases. The depth profiles of silicon are just the opposite to those of oxygen in Fig. 1(b). The oxygen–silicon ratios can also be figured out, as shown in Fig. 1(c). The oxygen–silicon ratio increases after oxygen ion implantation, and its shape is in agreement with the distribution of implanted oxygen ions. Figure 1(d) shows the depth distributions of displacement damage (dpa) in fused silica surface at different ion energies. The dpa represents the degree of damage to substrate caused by implanted ions. As we can see in Fig. 1(d), with the increase of the ion energy, the damage area broadens and extends from the surface to the inside. Based on the above results, the depth of implanted oxygen ions increases, the damage degree becomes more seriously with the increasing ion energy.

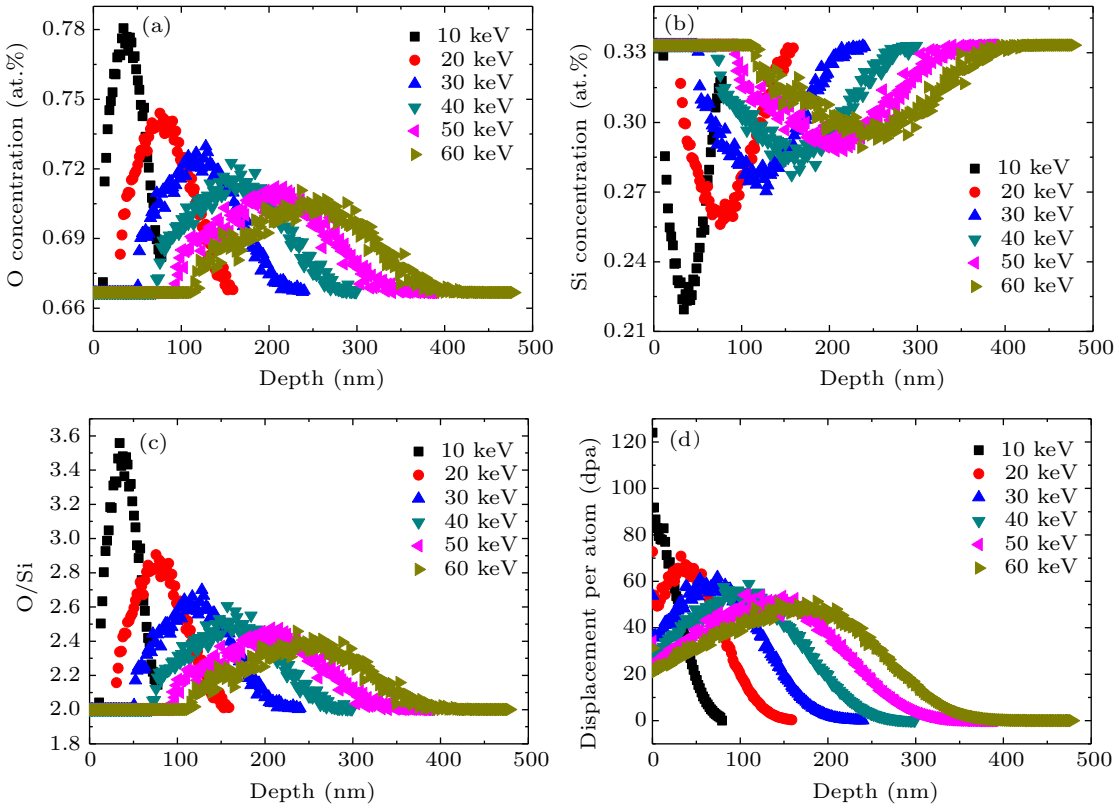


Fig. 1. Simulated results of O^+-implanted fused silica at different ion energies: (a) oxygen distributions; (b) silicon distributions; (c) oxygen-silicon ratios; (d) displacement damage distributions.

The oxygen profiles before and after ion implantation were obtained by TOF-SIMS, as shown in Fig. 2. It can be seen that the oxygen intensity of the O^+-implanted sample is higher than that of the un-implanted sample surface, which proves that oxygen ions have been implanted in the substrate, corresponding to the simulated results.

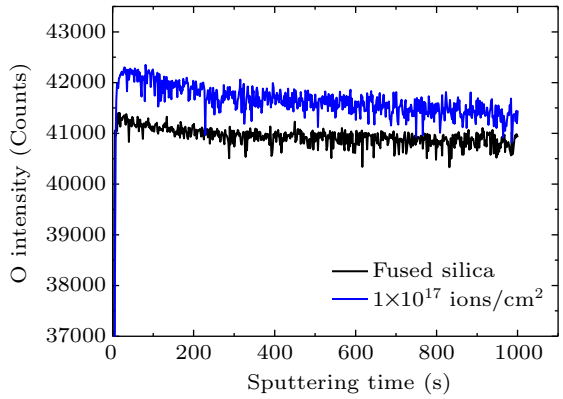


Fig. 2. The oxygen depth profiles of fused silica surfaces before and after oxygen ion implantation by TOF-SIMS.

3.2. Surface morphology and roughness

The microscopic morphologies of fused silica surfaces before and after oxygen ion implantations at different ion energies were measured by AFM, as shown Fig. 3. The average RMS surface roughness of O^+-implanted fused silica samples with various ion energies was calculated and the results are also shown in Fig. 3. Although all samples had been polished and cleaned, the impurity defects and sub-/surface defects still existed in fused silica surfaces. Therefore, the surface of un-implanted sample has a relatively large RMS roughness of 0.352 nm. According to Figs. 3(b)–3(d), the RMS roughness of the samples has a tendency of decrease when the ion energy increases from 10 keV to 30 keV. This change can be interpreted in terms of the sputtering effect accompanied with ion implantation which can remove the metal impurities and the residual polishing particles. At the same time, the sputtering effect can passivate the sub-/surface defects (scratch, upheaval, groove, etc.) to smooth these destructive defects. As a result, the sample surface roughness decreases and the surface quality becomes better. Subsequently, as the ion energy increases, ion implantation becomes dominant, and sputtering effect is weakened, which becomes the main factor affecting surface roughness. Therefore, the RMS roughness increases slightly to a stable value of 0.3 nm when the ion energy exceeds 40 keV. But the RMS roughness of the implanted sample surface is still lower than that of un-implanted sample surface. Generally, the sputtering effect during the oxygen ion implantation process can remove metal impurities and residual polishing particles, and passivate sub/-surface defects, thus improving the surface quality.

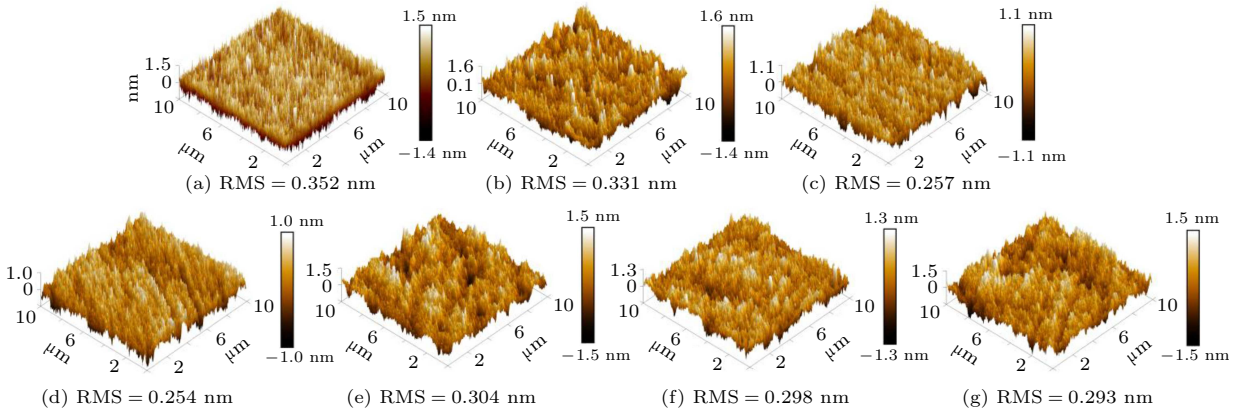


Fig. 3. AFM images of O^+-implanted fused silica at different ion energies: (a) 0 keV; (b) 10 keV; (c) 20 keV; (d) 30 keV; (e) 40 keV; (f) 50 keV; (g) 60 keV.

3.3. Structural defects

Fused silica has a three-dimensional grid framework with the basic tetrahedral structure composed of Si and O. In the fabrication of fused silica components, the abnormal distribution of oxygen atoms will lead to the formation of intrinsic structural defects such as oxygen vacancy defect (ODC), non bridged oxygen center (NBOHC), etc. Under the laser irradiation, these defects will become the strong absorption centers of ultraviolet laser energy, so that the temperature of the defect centers rises rapidly. This eventually leads to electron avalanche ionization, which destroys the structure of the material.[28]

In order to study evolution of structural defects of fused silica sample surfaces induced by oxygen ion implantation, the optical absorption spectra of the samples before and after oxygen ion implantation at various energies were measured and the results are shown in Fig. 4. As can be seen in Fig. 4, the un-implanted sample has two absorption peaks at 232 nm and 280 nm, corresponding to E′ centers and NBOHC, respectively.[8,29] The intensities of these absorption peaks decrease with the increasing ion energy and reach the minimum

at 30 keV. During the oxygen ion implantation, the implanted oxygen ions will combine with Si dangling bonds.[30] What's more, owing to the electronic effect caused by oxygen ion implantation, the E′ centers are combined with NBOHCs, resulting in the restoration of complete tetrahedral structure. Hence, the decrease of concentrations of E′ centers and NBOHC manifests as the decrease of the intensities of both two peaks. However, when fused silica is bombarded with high energy ions, a series of collisions between implanted ions and the native atoms will lead to the breaking of Si–O–Si bonds, forming the structural defects (E′ center, NBOHC, etc.).[13] Therefore, oxygen ion implantation can not only mitigate the structure defects, but also introduce defects into the surface. When the ion energy is larger than 30 keV, the defect production is greater than defect recombination, resulting in the increase of the concentrations of E′ centers and NBOHC. Therefore, the intensities of the absorption peaks of these two structural defects increase when the ion energy exceeds 30 keV.

In addition, the absorption edge is found to shift to the lower wavelength (blue shift) when the ion energy is below 50 keV, which reduces the possibility of multi-photon ionization and avalanche ionization of fused silica under 355 nm laser irradiation. As a consequence, the damage of fused silica caused by optical breakdown will be alleviated.

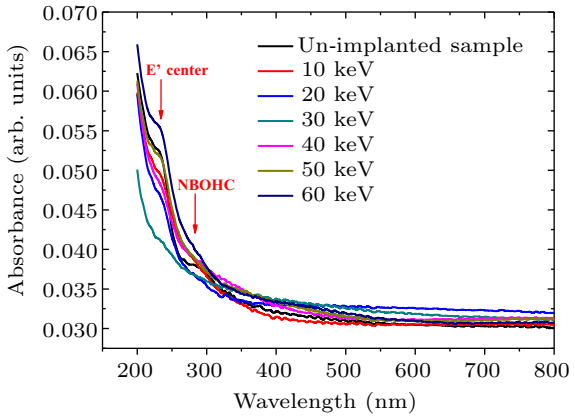


Fig. 4. Absorption spectra of O^+-implanted fused silica surfaces at different ion energies.

For better understanding the types and densities of the structural defects, the PL spectra of un-implanted and O^+-implanted fused silica sample surfaces were measured, as shown in Fig. 5. The PL spectrum of the un-implanted sample exhibits two peaks at ∼ 350 nm and ∼ 500 nm, corresponding to metallic impurities and oxygen-deficiency related defect (ODC), respectively.[31] The intensities of both peaks change with the ion energy, indicating that the densities of these defects are related to the ion energy. The intensity of the PL peak at 350 nm decreases and tends to be stable with increasing ion energy, indicating that the densities of metallic impurities decrease during the ion implantation process. This is attributed to the sputtering effect accompanied by ion implantation, corresponding to the result of AFM (in Fig. 2). The intensity of the strong and broad PL band at around 500 nm appears to reduce significantly when ion energy below 40 keV. It is because that the implanted oxygen ions will be captured by ODCs to combine, and the higher ion energy has a deeper distribution of the implanted oxygen ions to recombine more ODC defects.[20] Therefore, as the ion energy increases to 40 keV, the density of ODC reduces obviously.

A new peak at 660 nm appears in the PL spectra when ion energy reaches 50 keV, which is ascribed to NBOHC.[32] Ion implantation will lead to the breaking of Si–O–Si bond to form the E′ centers and NBOHCs. Meanwhile, the implanted oxygen ions can combine with E′ centers to form NBOHCs.[30] Both of them lead to the increase of the density of NBOHC defects. As the ion energy goes up to 60 keV, excessive energy will aggravate the breaking of Si–O bonds in substrate including NBOHCs. As a result, NBOHCs are transformed into E′ centers. Then two E′ centers can be combined into ODCs.[13] Therefore, the density of NBOHC decreases and the density of ODC increases obviously.

From the above experimental results analysis, it can be concluded that the process of oxygen ion implantation is accompanied by the formation and recombination of defects, leading to the absorption peak intensity varying with the ion energy. At the ion energy of 30 keV, due to the dynamic balance between the generation and recombination of defects, fused silica surface has the least defect types and the minimum defect density. The results indicate that oxygen ion implantation with appropriate ion energy conduces to eliminate or mitigate the structural defects of fused silica surface.

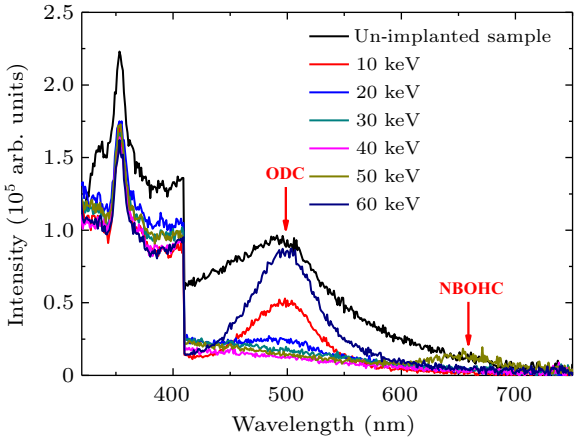


Fig. 5. PL spectra of O^+-implanted fused silica surfaces at different ion energies.

3.4. Micro structure

Infrared absorption spectrum is commonly used to study the changes of fused silica structure. Figure 6 shows the infrared absorption spectra of O^+-implanted fused silica sam-

ple surfaces at different implanted energies. In order to better understand the change of the absorption peak position, the overlapping peaks of samples were resolved into four Gaussian peaks centered at ∼ 787 nm, ∼ 982 nm, ∼ 1076 nm and ∼ 1179 nm, corresponding to the Si–O–Si bending vibration mode (TO_2), Si–OH bridging mode (υ_1), transverse optical mode (TO_3) and longitudinal optical mode (LO_3) of the Si–O–Si asymmetric stretching, respectively. The Gaussian peak positions of infrared absorption spectra of the sample surfaces before and after oxygen ion implantation are listed in Table 1. The shift of infrared absorption peak positions indicates that the molecular structures of fused silica surface are changed by oxygen ion implantation, which is mainly manifested by the change of Si–O–Si bond angle and material density, generally monitored by the TO_3 peak.[33] With the increase of the ion energy, the TO_3 peak continually shifts toward the lower wavenumber, indicating that the Si–O–Si bond angle decreases. This gives rise to the increase of surface density and the compaction of surface structure. Therefore, oxygen ion implantation can reduce the Si–O–Si bond angle and densify the surface structure of fused silica, leading to the formation of compressive stress which will enhance the fracture resistance of the fused silica surface.

Table 1. Positions of Gaussian peaks in infrared absorption spectra of fused silica before and after oxygen ion implantation.

Ion energy (keV)	Group vibration model			
	TO_2 (cm^{-1})	υ_1 (cm^{-1})	TO_3 (cm^{-1})	LO_3 (cm^{-1})
0	787.11	982.94	1076.17	1179.06
10	785.91	977.57	1072.18	1178.05
20	786.88	971.12	1066.99	1172.18
30	783.66	965.74	1062.19	1175.30
40	784.54	965.77	1061.11	1179.09
50	786.54	961.03	1052.85	1182.28
60	785.22	956.97	1049.05	1183.73

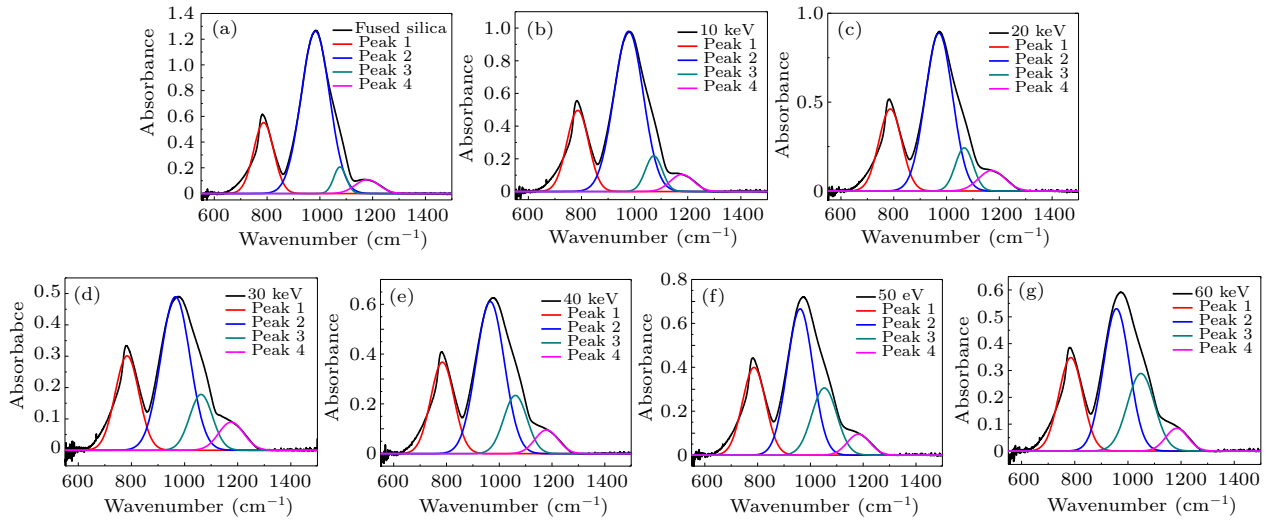


Fig. 6. Infrared absorption spectra of un-implanted and O^+-implanted fused silica at different ion energies.

3.5. Mechanical property

Nanoindentation technique has been widely used to measure mechanical properties of materials surface on the nanometer scale. In the past decade, researchers have made a systematic study on the measurement of surface stress by depth-sensing indentation technique and found that the compressive stress can restrain the plastic strain of the indentation while the tensile stress has an opposite effect.[34]

In order to investigate the mechanical properties of fused silica surfaces at different ion energies, the load–displacement curves of the sample surface with the maximum loading force of 5 mN are shown in Fig. 7. When the load is fixed, the displacement curves of loading and unloading will move to the left under the compressive stress generally, but it is opposite under the tensile stress.[35] Moreover, the offset of the curve increases with the increase of the stress. From Fig. 7, under the same load at 5 mN, the loading and unloading curves of O^+implanted sample surfaces shift to the left compared with that of the un-implanted sample surface. The result indicates that the oxygen ion implantation leads to the formation of compressive stress in the surface. The magnitude and distribution of the compressive stress are closely related to the oxygen ion distribution determined by the ion energy, which implies that the compressive stress may be resulted from the surface densification. At the fixed fluence of 1×10^{17} ions/cm^2, the higher ion energy will lead to the increase of ion implantation depth, indicating that the ion distribution is more dispersed, and the number ions implanted per unit volume in the sample surface is less, as shown in Fig. 1(a). Therefore, with the increasing ion energy, the compressive stress decreases, but the distribution depth of compressive stress increases. In fact, the oxygen ion implantation leads to a maximum compressive stress at 10 keV with the fixed ion fluence of 1×10^{17} ions/cm^2.

According to Oliver and Pharr's classical method for calculating the hardness and elastic modulus based on the load–displacement curve,[36] the hardness and elastic modulus of O^+-implanted fused silica surfaces at different ion energies under the maximum loading force of 5 mN are listed in Table 2. The hardness and elastic modulus increase in the O^+-implanted samples, and the changing trend with ion energy is the same as that of compressive stress, which confirms that the oxygen ion implantation with appropriate ion energy can strengthen the surface and improve the mechanical properties of fused silica surface resulting from the surface densification of the material.

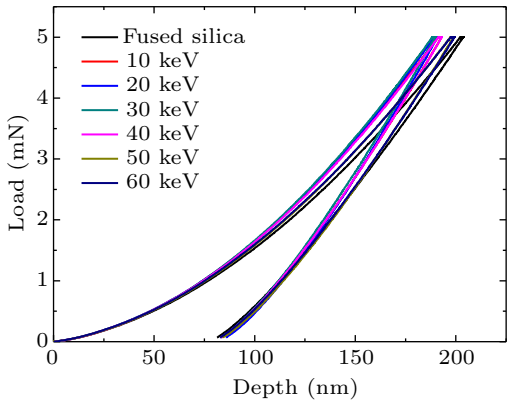


Fig. 7. Load–displacement curves of O^+-implanted fused silica surface at different ion energies under the maximum loading force of 5 mN.

Table 2. Hardness and elastic modulus of O^+implanted fused silica surface at different ion energies under the maximum loading force of 5 mN.

		Ion energy (keV)						
		0	10	20	30	40	50	60
$F_{max} = 5$ mN	Hardness, H (GPa)	7.91	8.29	8.35	8.36	8.28	8.15	8.08
	Elastic modolus, E (GPa)	55.63	65.11	67.86	68.03	64.98	60.67	59.71
	Final depth, d (nm)	203.75	192.91	190.91	189.90	193.07	198.79	199.38

3.6. Laser damage performance

The laser-induced damage thresholds of un-implanted and O^+-implanted fused silica at different ion energies were measured and the results are shown in Fig. 8. Before the ion implantation, the LIDT of the sample is 21.83 J/cm^2. In the process of ion implantation, the incident ions can remove the surface impurity defects and passivate the destructive defects, thus improving the surface quality. Besides, a tremendous amount of implanted oxygen ions combine with Si dangling bonds, leading to the reduction of ODC and the transformation from E′ center to NBOHC. Because of the electron effect accompanied by ion implantation, the E′ center and NBOHC are recombined into a complete Si–O–Si bond. All of these processes will result in the decrease of the densities of structural defects, which can reduce the absorption of UV laser energy. In addition, oxygen ion implantation can compact the surface structure, leading to the formation of compressive stress in the surface and the strengthening of the sample surface. As a result, as the ion energy increases, the LIDT gradually increases and reaches a maximum of 28.49 J/cm^2 at 30 keV, increasing by 30.51% compared with that of un-implanted samples. However, with the continuous increase of the ion energy, the surface roughness increases slightly and reaches a stable value. In addition, the excessive energy can break the Si–O bonds which will increase the density of structural defects. Moreover, the compressive stress decreases gradually and the surface strength decreases slightly. Hence, the LIDT gradually decreases to 23.09 J/cm^2 as the ion energy increases to 60 keV, which is still higher than that of un-implanted sample. This is because of the existence of compressive stress in the surface and the compensation for oxygen loss of the surface by implanted oxygen ions when the fused silica sample is irradiated by laser.

The damage growth of fused silica samples was investigated before and after oxygen ion implantation. The laser beam with laser energy density of 27 J/cm^2 was used to cause initial damage to the rear surface of fused silica samples, and then the damage growth was measured under the laser irradiation of 13.58 J/cm^2. The results show that the area of damage spot increases exponentially with the number of irradiation pulses, as shown in Fig. 9(a). The relationship between the area of the damage spots and the number of irradiation pulses can be expressed as

$$A = A_0 \, e^{\alpha N},$$

where A_0, N, A and α are the area of the initial damage spot, the number of irradiation pulses, the area of damage spot after N pulses laser irradiation and the damage growth coefficient, respectively. Therefore, the damage growth coefficients of un-implanted and O^+-implanted fused silica were obtained by calculation, as shown in Fig. 9(b).

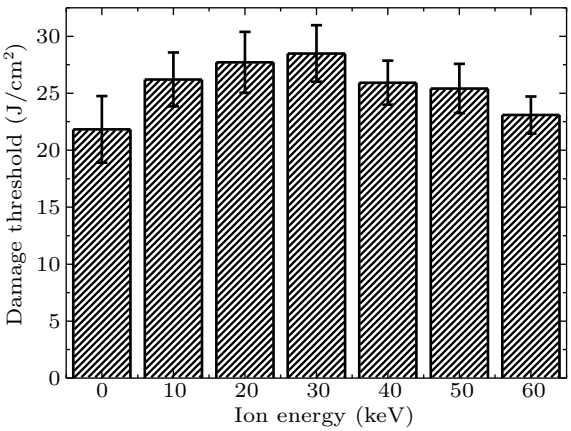


Fig. 8. Laser-induced damage thresholds of O^+-implanted fused silica at different ion energies.

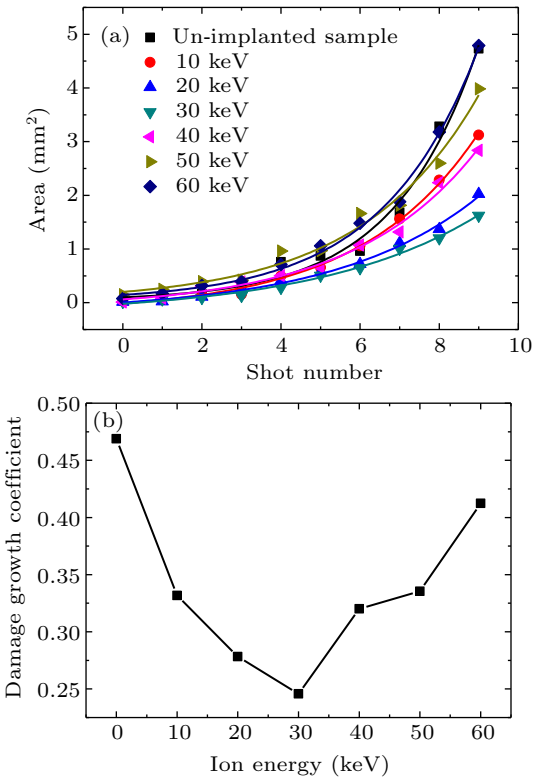


Fig. 9. Damage growth of O^+-implanted fused silica at different ion energies: (a) damage growth curves; (b) damage growth coefficient.

The removal of surface impurities and the passivation of sub-/surface defects reduce the laser-induced damage to the fused silica surface. In addition, the implanted oxygen ions can recombine the structural defects and compensate the loss of oxygen in fused silica surface under laser irradiation, which can reduce the absorption of laser energy and the plasma pressure in crack zone, thus relieving the crack propagation. Moreover, the compressive stress produced by oxygen ion implantation can counteract or eliminate the thermal stress induced by laser irradiation. Hence, the damage growth coefficient decreases with the increase of ion energy when the ion energy is below 30 keV. However, when the ion energy exceeds 30 keV, the slightly increase of surface roguness, the increase of structural defect density and the decrease of compressive stress will all lead to the increase of the damage growth coefficient.

In conclusion, the laser damage performance of fused silica is affected by various factors, including surface quality, defects and surface stress. After oxygen ion implantation with appropriate energy, the improvement of the surface quality, the recombination of the structural defects and the formation of the compressive stress are beneficial to increase the laser-induced damage thresholds and alleviate the damage growth.

4. Conclusion

Oxygen ions with different energies (10 keV–60 keV) at a fixed fluence (1×10^{17} ions/cm^2) were implanted into the fused silica surface. The effects of oxygen ion implantation on the surface morphology, micro-structure, mechanical properties and laser damage performance of fused silica surface were studied systematically. We have found that the sputtering effect accompanied with ion implantation can remove or passivate the sub-/surface defects (residual polishing particles, metal impurities, scratches, etc.) and reduce surface roughness to improve the surface quality slightly. The implanted oxygen ions can combine with oxygen-deficient structural defects to reduce the density of structural defects and compensate the loss of oxygen in fused silica surface under laser irradiation. Oxygen ion implantation also can reduce the Si–O–Si bond angle and increase the surface density, forming a compressive stress layer and strengthening the surface of fused silica. Therefore, when the ion energy is below 30 keV, the above synergistic effects enhance the laser-induced damage thresholds of fused silica and inhibit the damage growth. When the ion energy exceeds 30 keV, the laser damage performance is slightly degraded due to the slight increase of surface roughness, the increase of structural defect density and the decrease of compressive stress. Based on the above results, oxygen ion implantation can effectively enhance the laser resistant capacity of fused silica with optimized ion energy of 30 keV. The study on the mechanism of oxygen ion implanted into fused silica and its effect on the laser damage performance is useful to improve the laser loading capacity of fused silica component.

Acknowledgements

Project supported by the National Natural Science Foundation of China (Grant No. 12105037) and the Key Project of National Natural Science Foundation of China–China Academy of Engineering Physics Joint Foundation (Grant No. U1830204).

References

[1] Spaeth M, Manes K, Bowers M and Celliers P 2016 *Fusion Sci. Technol.* **69** 366
[2] Casner A, Caillaud T, Darbon S, Duval A, Thfoin I, Jadaud J P, Lebreton J P, Reverdin C, Rosse B, Rosch R, Blanchot N, Villette B, Wrobel R and Miquel J L 2014 *High Energy Density Phys.* **17** 2
[3] Zheng W, Wei X, Zhu Q, Jing F, Hu D, Su J, Zheng K, Yuan X, Zhou H, Dai W, Zhou W, Wang F, Xu D, Xie X, Feng B, Peng Z, Guo L, Chen Y, Zhang X, Liu L, Lin D, Dang Z, Xiang Y and Deng X 2016 *High Power Laser Sci. Eng.* **4** e21
[4] Bercegol H, Bouchut P, Lamaignere L, Garrec B Le and Raze G 2014 *Proc. SPIE* **5273** 312
[5] Neauport J, Cormont P, Lamaignere L, Ambard C, Pilon F and Bercegol H 2008 *Opt. Commun.* **281** 3802
[6] Feit M D and Rubenchik A 2004 *Proc. SPIE* **5273** 264
[7] Kucheyev S and Demos S 2003 *Appl. Phys. Lett.* **82** 3230
[8] Vaccaro L, Cannas M, Radzig V and Boscaino R 2008 *Phys. Rev. B* **78** 075421
[9] Menapace J A 2010 *Proc. SPIE.* **7842** 78421W
[10] Suratwala T, Miller P, Bude J, Steele W, Shen N, Monticelli M, Feit M, Laurence T, Norton M, Carr C and Wong L 2011 *J. Am. Ceram. Soc.* **94** 416
[11] Li B, Hou C, Tian C, Guo J, Xiang X, Jiang X, Liao W, Yuan X, Jiang X and Zu X 2019 *Appl. Surf. Sci.* **508** 145186
[12] Sun L, Liu H, Huang J, Ye X, Cheng Q, Zhou X, Wang F, Jiang X and Wu W 2013 *Proc. SPIE* **8786** 87860P
[13] Stevens-Kalceff M and Wong J 2005 *J. Appl. Phys.* **97** 113519

[14] Zheng Z, Zu X T, Zhang Y and Zhou W 2020 *Mater. Today Phys.* **15** 100262
[15] Xu S Z, Yuan X D, Zu X T, Lv H B, Jiang X L, Zhang L and Zheng W G 2007 *J. Non-Cryst. Solids* **353** 4212
[16] Stevens-Kalceff M, Stesmans A and Wong J 2002 *Appl. Phys. Lett.* **80** 758
[17] He J X, Shen Y, Li B, Xiang X, Li S, Fang X, Xiao H Y, Zu X T and Qiao L 2021 *Opt. Mater.* **111** 110611
[18] Silin A 1991 *Proc. SPIE* **1513** 270
[19] Derryberry S L, Weeks R A, Weller R A and Mendenhall M 1991 *Nucl. Instrum. Meth. B* **59–60** 1320
[20] Griscom D L 1985 *J. Non-Cryst. Solids* **73** 51
[21] Chinellato V, Gottardi V, Russo S Lo, Mazzoldi P, Nicoletti F and Polato P 1982 *Radiation Effects* **65** 31
[22] Idé J, Cornil D, Jacques A, Navet B, Boulanger P, Ventelon L, Lazzaroni R, Beljonne D and Cornil J 2019 *Adv. Theor. Simul.* **2** 1900039
[23] EerNisse E 1974 *J. Appl. Phys.* **45** 167
[24] Wang C Z, Wang H X, Krishna S, Morozov E V and Hazell P J 2021 *Thin-Walled Structures* **159** 107281
[25] Li B, Xiang X, Liao W, Han S, Yu J, Jiang X, Mushtaq M, Yuan X, Zu X and Fu Y 2019 *Appl. Surf. Sci.* **471** 786
[26] Felter T E, Hrubesh L, Kubota A Davila L and Caturla 2003 *Nucl. Instrum. Meth. B* **207(1)** 72
[27] Riede W, Willamowski U, Dieckmann M, Ristau D, Broulik U and Steiger B 1998 *Proc. SPIE* **3244** 96
[28] Glebov L B 2002 *Proc. SPIE* **4679** 321
[29] Pacchioni G and Ferrario R 1998 *Phys. Rev. B* **58** 6090
[30] Fitting H J, Barfels T, Trukhin A, Schmidt B, Gulans A and Czarnowski A 2002 *J. Non-Cryst. Solids* **303** 218
[31] Skuja L 1992 *J. Non-Cryst. Solids* **149** 77
[32] Skuja L 1994 *J. Non-Cryst. Solids* **179** 51
[33] Tomozawa M, Hong J W and Ryu S R 2005 *J. Non-Cryst. Solids* **351** 1054
[34] Zhu L N, Xu B S Xu, Wang H D and Wang C B 2015 *Crit. Rev. Solid State* **40** 77
[35] Lee Y and Kwon D 2003 *Scr. Mater.* **49** 459
[36] Pharr G M, Oliver W and Brotzen F R 1992 *J. Mater. Res.* **7** 613